Published in final edited form as:
*Am J Physiol Lung Cell Mol Physiol*. 2007 August ; 293(2): L417–L428. doi:10.1152/ajplung.00489.2006.

# $PGE_2$ inhibition of TGF-β1-induced myofibroblast differentiation is Smad-independent but involves cell shape and adhesion-dependent signaling

**Peedikayil E. Thomas**, **Marc Peters-Golden**, **Eric S. White**, **Victor J. Thannickal**, and **Bethany B. Moore**
Department of Internal Medicine, Division of Pulmonary and Critical Care Medicine, University of Michigan, Ann Arbor, Michigan

## Abstract

Myofibroblasts are pathogenic in pulmonary fibrotic disease due to their exuberant production of matrix rich in collagen that interferes with gas exchange and the ability of these cells to contract and distort the alveolar space. Transforming growth factor-β1 (TGF-β1) is a well-known inducer of myofibroblast differentiation. TGF-β1-induced transformation of fibroblasts to apoptosis-resistant myofibroblasts is adhesion-dependent and focal adhesion kinase (FAK)-mediated. Prostaglandin $E_2$ ($PGE_2$) inhibits this differentiation via E prostanoid receptor 2 (EP2) signaling and cAMP elevation, but whether $PGE_2$ does so by interfering with TGF-β1 signaling is unknown. Thus we examined the effects of $PGE_2$ in the presence and absence of TGF-β1 stimulation on candidate signaling pathways in human lung fibroblasts. We now demonstrate that $PGE_2$ does not interfere with TGF-β1-induced Smad phosphorylation or its translocation to the nucleus. Rather, $PGE_2$ has dramatic effects on cell shape and cytoskeletal architecture and disrupts the formation of appropriate focal adhesions. $PGE_2$ treatment diminishes TGF-β1-induced phosphorylation of paxillin, STAT-3, and FAK and, in turn, limits activation of the protein kinase B (PKB/Akt) pathway. These alterations do not, however, result in increased apoptosis within the first 24 h of treatment. Interestingly, the effects of $PGE_2$ stimulation alone do not always mirror the effects of $PGE_2$ in the presence of TGF-β1, indicating that the context for EP2 signaling is different in the presence of TGF-β1. Taken together, our results demonstrate that $PGE_2$ has the potential to limit TGF-β1-induced myofibroblast differentiation via adhesion-dependent, but Smad-independent, pathways.

### Keywords

fibrosis; eicosanoid; lung; signal transduction

Smooth Muscle Actin-α (α-SMA) expression (39), stress fiber formation (25), and robust collagen secretion are the distinguishing features of myofibroblasts. The multifunctional cytokine, transforming growth factor-β1 (TGF-β1), is a well-characterized profibrotic mediator (2,3) that induces transformation of fibroblasts to myofibroblasts both in vitro (7) and in vivo (36). Myofibroblasts display contractile properties intermediate between smooth muscle cells and fibroblasts and appear transiently in the granulation phase of normal wound healing to provide the contractile force required for wound closure (6,38). Eventual apoptosis of fibroblasts/myofibroblasts is essential for normal repair and resolution of tissue scarring.



Address for reprint requests and other correspondence: B. B. Moore, Univ. of Michigan, Dept. of Internal Medicine, Division of Pulmonary and Critical Care Medicine, 4062 BSRB, 109 Zina Pitcher Pl., Ann Arbor, MI 48109-2200 (bmoore@umich.edu).

Myofibroblast differentiation and activation by TGF-β1 is a critical event in the pathogenesis of human fibrotic diseases, since TGF-β1 not only causes the differentiation of fibroblasts to myofibroblasts, but also renders myofibroblasts resistant to apoptosis by activating phosphatidylinositol 3-kinase (PI3K)/Akt signaling (15). In turn, activated Akt induces the prosurvival NF-κB pathway (33,44). Prolonged persistence of myofibroblasts at the site of injury leads to fibrosis and progressive organ dysfunction of lung, kidney, and other tissues. TGF-β1-induced differentiation of fibroblasts to myofibroblasts is dependent on cell adhesion and integrin signaling involving focal adhesion kinase (FAK) (41). We (21) previously showed that this TGF-β1-mediated differentiation process is inhibited by prostaglandin $E_2$ ($PGE_2$) via E prostanoid receptor 2 (EP2) signaling and cyclic adenosine monophosphate (cAMP) elevation. $PGE_2$ could potentially block any of the well-known signal transduction events that occur as a result of TGF-β1 stimulation in fibroblasts. The best known pathway for TGF-β1 signaling in fibroblasts includes Smad phosphorylation and translocation to the nucleus followed by binding of nuclear Smad complexes to the Smad-binding elements (SBEs) of target genes. The ability of Smads to regulate gene transcription further depends on the presence of transcriptional coactivators such as p300 (1).

TGF-β1 also acts through Smad-independent but adhesion-dependent pathways. FAK is a cytoplasmic nonreceptor protein tyrosine kinase found in focal adhesions of cells with extracellular matrix, and its activity is regulated by ligand binding to cell surface receptors including the integrins (27). The focal adhesion complex is involved in the regulation of cell shape, function, survival, migration, and signaling. The effects of $PGE_2$ on fibroblast cell morphology, adhesion, FAK phosphorylation, and Akt activation remain obscure.

The research presented in this manuscript identifies potential mechanisms whereby $PGE_2$ counteracts TGF-β1 signaling in human lung fibroblasts. Our results indicate for the first time that $PGE_2$ effects are independent of Smad and that $PGE_2$ disrupts the normal formation of TGF-β1-induced focal adhesions and also identify several potential signaling targets for $PGE_2$ downstream from TGF-β1.

## MATERIALS AND METHODS

### Cell culture and reagents

This study was approved by the University of Michigan Institutional Review Board. All experiments were performed on early passage normal human lung fibroblasts (IMR-90; Institute for Medical Research, Camden, NJ) or primary fibroblasts grown from histologically normal-appearing lung from patients undergoing resection for pulmonary nodules. Adult fibroblasts were the kind gift of Dr. Cory Hogaboam at our institution. IMR-90 cells were maintained in a medium consisting of Dulbecco's modified Eagle's medium (BioWhittaker, Walkersville, MD) supplemented with 10% fetal calf serum (Sigma, St. Louis, MO), 100 U/ml penicillin/streptomycin, and Fungizone (GIBCO, Grand Island, NY). Adult lung fibroblasts were maintained in medium containing 15% serum. Medium was changed every 3 days, and cells were expanded and plated onto 35- and 100-mm dishes. At 85% confluency, cells were growth-arrested by reducing the concentration of fetal calf serum in the medium to 0.01% for 48 h before stimulation with porcine platelet-derived TGF-β1 (2 ng/ml; R&D Systems, Minneapolis, MN) and/or $PGE_2$ (generally at 10 nM unless otherwise indicated; Cayman Chemicals, Ann Arbor, MI). The concentration of $PGE_2$ used in the adult lung fibroblasts was generally 100 nM based on our previous dose response studies (21). Forskolin, a direct activator of adenylyl cyclase used at 100 μM, was from Sigma. Butaprost, an EP2 receptor agonist, was obtained from Cayman Chemicals and used at 5 μM.

### Western blotting

Cells grown on tissue culture plates were washed with phosphate-buffered saline (PBS) and lysed in 0.5 ml of ice-cold RIPA lysis buffer (1% sodium deoxycholate, 0.1% SDS, 0.15 M NaCl, 0.01 M $NaH_2PO_4$, 2 mM EDTA, 0.5 mM NaF) containing 2 mM sodium orthovanadate and 1:100 dilution of protease inhibitor mixture III (Calbiochem). Protein concentrations were determined using the DC protein assay reagents from Bio-Rad (Hercules, CA). SDS-PAGE and Western blot analyses were performed as described previously (14,21).

### Subcellular fractionation

IMR-90 cells treated with or without $PGE_2$ and/or TGF-β1 for 5 min, 30 min, or 24 h were washed with cold PBS and harvested by mechanical detachment with a rubber policeman in a buffer containing 10 mM Tris ·HCl, pH 7.5, 0.32 M sucrose, 3 mM $CaCl_2$, 2 mM magnesium acetate, 0.1 mM EDTA, 1 mM dithiothreitol (DTT), and 0.5% Nonidet P-40. Cell suspensions were then homogenized with a Tissue-Tearor (Biospec Products) and centrifuged at 5,000 *g* for 10 min at 4°C. To isolate nuclei, the pellets were layered over sucrose gradient buffer containing 1.7 M sucrose, 5 mM magnesium acetate, 0.1 mM EDTA, and 10 mM Tris ·HCl, pH 8.0, followed by centrifugation at 30,000 *g* for 45 min at 4°C. The 5,000 *g* postnuclear supernatant was centrifuged at 105,000 *g* for 1 h. The pellet was collected as membrane fraction and the supernatant as cytosol. Pellets of nuclei and membrane were suspended in RIPA buffer. Nuclear, membrane, and cytosol fractions were boiled with 6×SDS electrophoresis sample buffer (0.35 M Tris ·HCl, pH 6.8, 30% glycerol, 10% SDS, 0.6 M DTT, 0.2% bromophenol blue).

### Antibodies

Sources for the antibodies used in this study were as follows. From Cell Signaling (Danvers, MA): phosphorylated Akt (p-Akt; S-473), Akt rabbit polyclonal, p-paxillin (Y-118) rabbit polyclonal, p-Smad2 (S-465/467), p38 MAP kinase rabbit polyclonal, p-p38 MAP kinase (T-180/Y182) mouse antibody, p-p44/42 MAP kinase rabbit polyclonal, p44/42 rabbit polyclonal, p-JNK rabbit polyclonal, p-p38 MAP kinase rabbit polyclonal, JNK rabbit monoclonal, p38 MAP kinase rabbit polyclonal, p-Y705-STAT-3 rabbit polyclonal, STAT-3 rabbit polyclonal. From Santa Cruz (Santa Cruz, CA): Smad4 mouse monoclonal. From BioSource (Carlsbad, CA): p-FAK (Y-397) rabbit polyclonal, FAK (H-1) mouse monoclonal, lamin A/C mouse monoclonal. From CedarLane (Burlington, NC): rabbit anti-human type I collagen polyclonal. From Sigma: β-actin mouse MAb, paxillin MAb. From Zymed (Carlsbad, CA): Smad3 and Smad2 rabbit polyclonals. From DakoCytomation: α-SMA clone 1A4 mouse monoclonal. From BioSource International (Camarillo, CA): pY397-FAK rabbit polyclonal. From Pierce Biotechnology (Rockford, IL): goat anti-mouse IgG peroxidase conjugate and goat anti-rabbit IgG peroxidase conjugate. pSmad3 rabbit antiserum was a gift from Dr. Ed Leof (Mayo Foundation, Rochester, MN).

### Morphological analysis and immunofluorescent staining

IMR-90 cells or normal adult lung fibroblasts were plated onto 35-mm dishes, grown to 50% confluence, growth-arrested for 48 h, and treated with or without TGF-β1 and/or $PGE_2$ or butaprost from 5 min to 24 h. Cells were washed with ice-cold PBS, fixed in cold methanol for 20 min, and blocked for 1 h in 3% BSA in PBS. Cells were incubated with anti-paxillin MAb (1:50 in 1% BSA/PBS) for 1 h and washed three times with PBS. Indocarbocyanine (Cy3)-conjugated secondary anti-mouse IgG (1:100) and FITC-phalloidin were added to the cells and incubated for 30 min. The cells were washed three times, and their nuclei were stained with ProLong Gold mounting medium containing 4,6-diamidino-2-phenylindole (DAPI; Invitrogen, Carlsbad, CA). Images were then captured using an Olympus FV500 laser-scanning

confocal microscope with a ×60 water immersion objective. Z-stack analysis confirmed the colocalization of the FITC and Cy3 signals in focal adhesions.

### Densitometry measurements

To determine the intensity of each band on Western blots, blots were scanned, and bands were analyzed for pixel density using the Image-J program available for download at http://rsb.info.nih.gov/ij/download.html.

### Statistical analysis

When three or more groups were analyzed, the data were analyzed by ANOVA with a post hoc Dunnet or Bonferroni examination; $P$ values <0.05 were considered to be statistically significant.

## RESULTS

### $PGE_2$ is able to limit TGF-β1-induced collagen and α-SMA expression

Our (15,21) previous results with IMR-90 cells have demonstrated that 2 ng/ml TGF-β1 induces robust fibroblast-to-myofibroblast transformation within 24 h. In addition, we (Ref. 21 and unpublished observations) have previously demonstrated that a dose response of $PGE_2$ ranging from 10 nM to 100 μM is able to limit TGF-β1-induced expression of both collagen 1 and α-SMA at 24 h. The ability of $PGE_2$ to limit collagen and α-SMA was similar across all concentrations. Thus we chose the lowest effective dose of $PGE_2$ (10 nM) for future experiments unless otherwise indicated. Interestingly, however, $PGE_2$ is able to activate cAMP production in fibroblasts very rapidly (5–15 min; Ref. 21). To determine whether $PGE_2$ was able to inhibit the TGF-β1-induced expression of either collagen 1 or α-SMA at an earlier time point, we cultured IMR-90 human lung fibroblasts in the presence or absence of TGF-β1 ± 10 nM $PGE_2$ for 5 min, 30 min, or 24 h. Figure 1*A* demonstrates that collagen 1 levels were decreased by $PGE_2$ (within 30 min), whereas the downregulation of α-SMA occurred later (24 h; Fig. 1, *A* and *B*). To determine whether $PGE_2$ alone had any effect on the basal expression of α-SMA or collagen 1, we compared the expression of these proteins in IMR-90 cells that had been stimulated with serum-free media alone, $PGE_2$ alone, TGF-β1 alone, or TGF-β1 + $PGE_2$ for 24 h (Fig. 1*B*). $PGE_2$ was able to inhibit both basal and TGF-β1-induced expression of collagen and α-SMA, although the inhibition was more pronounced in the presence of TGF-β1.

### $PGE_2$ did not affect the TGF-β1-stimulated phosphorylation of Smad2/3

TGF-β1 is known to induce the phosphorylation of the transcription factors Smad2 and Smad3 that are involved in collagen synthesis (10,29). Hence, we investigated the effect of $PGE_2$ signaling on TGF-β1-induced Smad phosphorylation (Fig. 2*A*). TGF-β1 induced phosphorylation of Smad2 and Smad3 in 30 min. $PGE_2$ (10 nM) did not have any effect on the phosphorylation of either Smad2 or Smad3 at any time point tested (Fig. 2*A*). Even doses of $PGE_2$ as high as 50 μM showed no inhibition of Smad phosphorylation (Fig. 2*B*) despite the fact that we (21) have previously shown these concentrations inhibit α-SMA expression. Thus these data suggest that the inhibitory effects of $PGE_2$ are independent of Smad2/3 phosphorylation.

### Translocation of Smad2/3/4 complex to the nucleus by TGF-β1 is not abrogated by $PGE_2$ treatments

Phosphorylated Smads are known to form Smad2/3/4 heteromeric complexes, which translocate to the nucleus to regulate the transcriptional machinery by binding to Smad-binding enhancer elements (26). Therefore, we determined whether the TGF-β1-induced translocation

of Smad complexes in myofibroblasts was blocked by $PGE_2$ treatment. We prepared nuclear and cytosolic fractions from IMR-90 cells treated with TGF-β1 with or without $PGE_2$. There was no decrease in the proportion of Smad2/3/4 in the nucleus or increase in the fraction of Smad2/3/4 found in the cytosol of cells treated with both TGF-β1 and $PGE_2$ compared with cells treated with TGF-β1 only (Fig. 2*C*). Thus we conclude that $PGE_2$ treatment did not interfere with the translocation of Smad2/3/4 complexes to the nucleus.

### TGF-β1 and $PGE_2$ cause sudden and sustained morphological changes

Differential morphological changes were noted in cells stimulated with TGF-β1 and/or $PGE_2$. Both untreated (control) and TGF-β1-treated cells were flat and spindle-shaped (Fig. 3*A*). In contrast, addition of 10 nM $PGE_2$ induced a rapid change (within 5 min) in the morphology of cultured lung fibroblasts (Fig. 3*A*). The spindle-shaped cells narrow and become irregular, and the cells appear shrunken in size. The surface area of cell attachment with fibrillar and focal adhesions also decreases. The vertical height of the cell appears to be increased in the middle compared with the flattened control cells. These effects of $PGE_2$ on fibroblast cell shape were concentration dependent, being even more pronounced at higher concentrations (data not shown). $PGE_2$ in the presence of TGF-β1 induces a morphology that is intermediate between that of cells treated with TGF-β1 alone and $PGE_2$ alone. The adenylyl cyclase activator, forskolin, at 100 μM concentration, was able to mimic the rapid change in cell shape induced by 10 nM $PGE_2$ (data not shown). The rapid morphological changes seen with $PGE_2$ alone were also noted in the presence of TGF-β1. Thus these data suggest that $PGE_2$ stimulation of cAMP induces rapid changes in fibroblast cell shape both in the presence and absence of TGF-β1.

### $PGE_2$ alters cytoskeletal structure

To determine what effect $PGE_2$ stimulation would have over a longer period of time, growth-arrested IMR-90 cells, treated with or without TGF-β1 and/or $PGE_2$ for 24 h, were methanol-fixed and stained with phalloidin for the visualization of actin stress fibers. Immunofluorescence of paxillin and phalloidin was used to visualize focal adhesions (Fig. 3*B*). Actin stress fibers (green) and focal adhesions (yellow/orange) were well-organized in TGF-β1-treated IMR-90 lung fibroblasts. Note that in TGF-β1-treated cells, the focal adhesions were dispersed along the stress fibers stretching toward opposite poles of the cell. In contrast, actin stress fibers and focal contacts were disorganized with totally distorted cell structure in cells treated with $PGE_2$ or both TGF-β1 and $PGE_2$ simultaneously. Although paxillin staining was evident in the $PGE_2$-treated samples, it was localized near the nucleus and was not found in characteristically dispersed focal adhesions. The changes noted in the TGF-β1 + $PGE_2$ treatment groups were intermediate between those of TGF-β1 alone or $PGE_2$ alone. Of note, treatment of the cells with an EP2 receptor agonist, butaprost alone, or in combination with TGF-β1 mimicked the effects of $PGE_2$ treatment. Thus $PGE_2$ likely acting through EP2 limits cytoskeletal changes normally associated with myofibroblast transformation by TGF-β1.

### $PGE_2$ inhibits TGF-β1-induced paxillin phosphorylation

We next investigated whether the cell shape changes induced by $PGE_2$ stimulation correlated with diminished phosphorylation of paxillin. Paxillin was phosphorylated on Y-118 at baseline in untreated cells, but TGF-β1 significantly enhanced Y-118 phosphorylation of paxillin within 30 min, and this response was maximal at 24 h. $PGE_2$ was able to inhibit paxillin phosphorylation in the presence of TGF-β1 at both the 30-min and 24-h time points (Fig. 4, *A* and *C*). Interestingly, however, $PGE_2$ increased the paxillin phosphorylation at shorter time periods when added alone (Fig. 4, *B* and *D*). Thus the rapid changes in cytoskeletal architecture that are seen with $PGE_2$ stimulation alone are not due to changes in paxillin phosphorylation per se, but rather diminished paxillin phosphorylation could contribute to the cell shape changes

that take place in the presence of TGF-β1 + $PGE_2$. As demonstrated by the immunohistochemistry data in Fig. 3, the organization of paxillin into appropriately distributed focal adhesions on stress fibers is also disrupted in the presence of $PGE_2$.

### $PGE_2$ limits TGF-β1-induced phosphorylation of STAT-3

Because STAT-3 has been shown to associate with paxillin and FAK in focal adhesions (35), we next tested the ability of $PGE_2$ cotreatment to limit STAT-3 phosphorylation. TGF-β1 treatment alone significantly induces STAT-3 phosphorylation within 5 min. However, $PGE_2$ cotreatment was able to block tyrosine phosphorylation of STAT-3 by the 30-min time point (Fig. 5, *A* and *C*). Thus diminished phosphorylation of both paxillin and STAT-3 likely contributes to the disruption of cytoskeletal interactions with focal adhesion complexes in the presence of both TGF-β1 and $PGE_2$. Interestingly, when STAT-3 phosphorylation was examined in response to $PGE_2$ alone, $PGE_2$ induced rapid phosphorylation of STAT-3 (5–30 min), but this was diminished by 24 h. These results suggest that the context for $PGE_2$ signaling is different in the presence and absence of TGF-β1.

### $PGE_2$ inhibits TGF-β1-stimulated Y-397 FAK autophosphorylation

We (41) previously demonstrated that the TGF-β1-induced differentiation of fibroblasts to myofibroblasts is dependent on cell adhesion and integrin signaling involving FAK. Since the focal adhesion-cytoskeletal architecture was distorted by $PGE_2$ treatment, we examined the effects of $PGE_2$ on TGF-β1-mediated FAK autophosphorylation (Fig. 6). FAK exhibited basal levels of autophosphorylation that were increased by 24 h with TGF-β1 treatment. $PGE_2$ was able to inhibit FAK autophosphorylation in the presence of TGF-β1 at all time points. $PGE_2$ also decreased the FAK autophosphorylation between 5–30 min when cultured alone and the inhibition was sustained. These data mirror the results seen with paxillin and suggest that signaling cascades induced by $PGE_2$ are different in the presence and absence of TGF-β1. Given that we (41) have previously demonstrated that expression of a dominant negative FAK construct can inhibit myofibroblast differentiation in IMR-90 cells, our current data link the effects of $PGE_2$ to the inhibition of FAK activation. Thus these results suggest that $PGE_2$ may disrupt myofibroblast transformation at least, in part, by limiting FAK signaling.

### $PGE_2$ inhibits TGF-β1-stimulated PKB/Akt phosphorylation

We (15) previously showed that TGF-β1 stimulated activation of the prosurvival PI3K/Akt pathway in human fibroblasts. Treatment of IMR-90 cells with TGF-β1 induced the S-473 phosphorylation of Akt in 5 min, and this phosphorylation increased with the duration of treatment through 24 h (Fig. 7). $PGE_2$ cotreatment inhibited the Akt phosphorylation at 30 min and 24 h. Interestingly, $PGE_2$, when added alone, could inhibit Akt phosphorylation at all time points. Thus the inhibition of Akt signaling by $PGE_2$ is TGF-β1 independent. We next assessed whether these alterations in Akt activation would result in differences in cell survival over the 24-h culture period by examining cell extracts for the presence of cleaved caspase-3 under all conditions. Despite the alterations in Akt induced by $PGE_2$ administration, there were no differences in the expression of cleaved caspase-3 (data not shown) under any conditions up to 24 h.

### $PGE_2$ signaling alters the kinetics of MAP kinase activation

Many signal transduction pathways involve phosphorylation and activation of one or more MAP kinases (9). TGF-β1 stimulation of fibroblasts is known to induce phosphorylation of p38 (12,15,20,40) and both ERK1/2 (12) and JNK (12,40). Thus we wanted to determine the effect of $PGE_2$ treatment on the phosphorylation of MAP kinases. With respect to ERK1/2 activation, TGF-β1 alone induced phosphorylation of ERK1/2 within 5 min, and the effect was increased at 30 min and sustained through 24 h (Fig. 8, *A* and *B*). TGF-β1-induced JNK

activation was maximal at 30 min, and this was the time point for maximal inhibition by $PGE_2$ as well (Fig. 8, *A* and *C*). The phosphorylation of p38 by TGF-β1 alone was slower, taking 24 h (Fig. 8, *A* and *D*), and $PGE_2$ did not inhibit this response at any time point. In all cases, $PGE_2$ coadministration with TGF-β1 altered the kinetics of MAP kinase activation. In the presence of TGF-β1 + $PGE_2$, all three kinases were activated within 5 min to a level higher than that seen with TGF-β1 alone. At later time points, $PGE_2$ inhibited the TGF-β1-induced phosphorylation of ERK1/2 and JNK but not p38. The kinetics of MAP kinase activation in the presence of $PGE_2$ alone also showed rapid activation of all three kinases within 5 min (Fig. 9). The ability of $PGE_2$ alone to limit kinase activation at 24 h, however, was kinase specific.

### $PGE_2$ and butaprost disrupt cell shape and focal adhesion formation in adult lung fibroblasts

To determine whether $PGE_2$ could alter the cellular morphology and formation of focal adhesions in adult lung fibroblasts, we cultured fibroblasts from peripheral adult lung demonstrated to be histologically normal. Adult fibroblasts were growth-arrested for 48 h, treated with or without TGF-β1 and/or $PGE_2$ or butaprost for 24 h, methanol-fixed, and stained with phalloidin for the visualization of actin stress fibers and paxillin. Colocalized immunofluorescence of paxillin and phalloidin was used to identify focal adhesions (Fig. 10). Similar to the results with fetal fibroblasts, TGF-β1 strongly stimulated the formation of stress fibers and dispersed focal adhesions. In contrast, treatment with $PGE_2$ alone or in combination with TGF-β1 distorted cell shape and limited the formation of focal adhesions. Butaprost treatment showed similar changes as $PGE_2$, although in the adult fibroblasts, the effects of butaprost were not as dramatic as the results in fetal fibroblasts. Thus $PGE_2$ is able to limit TGF-β1-induced cytoskeletal changes in both fetal and adult lung fibroblasts.

### $PGE_2$ inhibits TGF-β1-induced Y-397 FAK autophosphorylation in adult lung fibroblasts

To determine whether the disruption of focal adhesion formation in adult fibroblasts correlated with an inhibition of FAK autophosphorylation, adult lung fibroblasts were serum-starved and cultured in the presence or absence of TGF-β1 and/or 100 nM $PGE_2$ for periods of 5 min, 30 min, or 24 h. TGF-β1 was able to stimulate FAK autophosphorylation within 30 min in normal adult fibroblasts, and $PGE_2$ was able to significantly inhibit this activation at the 24-h time point (Fig. 11). Thus $PGE_2$ is able to limit the formation of focal adhesions and the activation of FAK in both fetal and adult fibroblasts.

## DISCUSSION

Fibroblasts and myofibroblasts are essential and transient participants in wound closure and repair, but persistence of myofibroblasts at the site of injury promotes dysregulated repair processes leading to fibrosis. The multifunctional cytokine, TGF-β1, induces the transformation of fibroblasts to apoptosis-resistant myofibroblasts with enhanced extracellular matrix synthetic capacity. Since the signals leading to the disappearance of myofibroblasts by massive apoptosis (8) in the final stages of wound healing are unknown, investigation of signals involved in $PGE_2$ inhibition of TGF-β1-induced myofibroblast transformation may shed light on these events and support new therapeutic strategies for prevention and treatment of fibrotic diseases. This is particularly true for lung fibrosis, since lung fibroblast activation is downregulated by $PGE_2$ (21,28,46) and since fibroblasts isolated from fibrotic lung show deficits in $PGE_2$ synthesis (19,43,47) and reduced expression of cyclooxygenase-2 (42,47). Animal models of fibrosis have also been shown to be modulated by $PGE_2$ levels. Fibrosis is worse in situations characterized by underproduction of $PGE_2$ (5,13) or diminished $PGE_2$ signaling (28). In contrast, situations resulting in enhanced $PGE_2$ production are often protective for fibrosis (32). Thus therapeutic administration of $PGE_2$ or EP2 agonists may improve fibrosis by limiting prosurvival signaling in myofibroblasts and/or by interfering with myofibroblast contraction and extracellular matrix synthesis. We (15) previously demonstrated

that adhesion/integrin-dependent autophosphorylation and activation of FAK (41) as well as activation of Akt are required for the induction of myofibroblast differentiation by TGF-β1. This differentiation to myofibroblasts is inhibited by $PGE_2$ via EP2 prostanoid receptor signaling and cAMP elevation (21). Our current research explores the signaling mechanisms that account for the ability of $PGE_2$ to limit myofibroblast transformation induced by TGF-β1. We demonstrate that $PGE_2$ inhibition of myofibroblast transformation is Smad independent. In contrast, $PGE_2$ appears to modulate the adhesion-dependent pathways involved in TGF-β1-induced myofibroblast differentiation including paxillin, STAT-3, FAK, and Akt. These data link the inhibition of myofibroblast differentiation by $PGE_2$ to the inhibition of FAK and corroborate our (41) earlier work demonstrating that interruption of FAK signaling can limit myofibroblast differentiation. Importantly, the current work demonstrates these relationships in both fetal and adult lung fibroblasts.

TGF-β1 signaling in fibroblasts is known to involve phosphorylation of Smad2 and Smad3 followed by association with Smad4. The trimeric Smad2/3/4 complex then translocates to the nucleus to induce transcription via binding to SBE elements in the promoters of target genes. In the case of myofibroblasts, it is interesting to note that $PGE_2$ inhibition of TGF-β1-induced collagen secretion appears to occur earlier than $PGE_2$ inhibition of α-SMA expression. This may reflect the fact that different, but perhaps overlapping, signaling pathways are involved in the regulation of these two genes. Smad2/3/4 does not generally initiate transcription alone but requires transcriptional coactivators such as CBP/p300. These cofactors may induce acetylation of the Smad complex to activate DNA binding (37). The ability of TGF-β1 to activate Smad signaling is adhesion independent (41). Because most TGF-β1-responsive genes are regulated in a Smad-dependent manner, we were surprised to discover that $PGE_2$ inhibition of myofibroblast differentiation was Smad independent. Cotreatment of IMR-90 cells with both TGF-β1 and $PGE_2$ had no effect on the phosphorylation of Smad2 and Smad3 and had no effect on the translocation of Smad2/3/4 to the nucleus compared with treatment with TGF-β1 alone. This was true even at very high concentrations of $PGE_2$. Thus $PGE_2$ did not appear to limit Smad phosphorylation or nuclear translocation. We did not, however, examine the acetylation status of the Smad complexes in our studies. We do not yet know whether $PGE_2$ treatment induces the expression of a transcriptional repressor or sequestration of CBP/p300 or whether $PGE_2$ functions merely by disrupting normal TGF-β1 signaling pathways.

Myofibroblast differentiation by TGF-β1 and the inhibition of that differentiation by $PGE_2$ were accompanied by changes in cell shape, cell adhesion to the matrix (fibrillar and focal adhesions), and cytoskeletal organization. Paxillin is a cytoskeletal protein found predominantly at focal adhesions and in the cytosol. Immunofluorescent staining of paxillin and actin stress fibers demonstrated dramatic alterations in focal adhesion, cytoskeletal structure, and cell shape induced by $PGE_2$ signaling in human fibroblasts. When added simultaneously, $PGE_2$ diminished TGF-β1-mediated Y-118 phosphorylation of paxillin and tyrosine-phosphorylation of STAT-3 at 30 min and 24 h. This was associated with dramatic loss and/or redistributions of focal adhesions within the treated cells. Cell shape changes associated with alterations in cytoskeletal structures and cell adhesions have been reported in human macrophages (34), murine Y1 adrenal cells (11), and rat vascular smooth muscle cells (31) by elevation in cAMP and in human aortic smooth muscle cells by prostacyclin analogs and $PGE_2$ (4). Microinjection of the catalytic subunit of PKA into living fibroblasts or the treatment of these cells with dibutyryl cAMP caused reversible alterations in cell morphology and complete loss of actin microfilament bundles (23). We (21) previously demonstrated that $PGE_2$ stimulation induces rapid cAMP elevations in IMR-90 cells. We have confirmed that $PGE_2$ stimulation alone activates the cAMP-responsive transcription factor CREB within 5 min in both IMR-90 cells and primary adult fibroblasts (data not shown and Ref. 16). $PGE_2$ decreases the Y-397 autophosphorylation of FAK when added in the absence of TGF-β1 between 5–30 min in IMR-90 cells, and this inhibition is sustained. FAK inhibition in adult

lung fibroblasts treated with $PGE_2$ in the presence or absence of TGF-β1 occurs by 24 h. Thus cAMP elevations are not sufficient to induce FAK activation in lung fibroblasts. Interestingly, $PGE_2$ is able to rapidly phosphorylate STAT-3 and paxillin when added alone. In contrast, $PGE_2$ signaling inhibits STAT-3 and paxillin activation in the presence of TGF-β1. These results clearly demonstrate that $PGE_2$ signaling differs in the presence and absence of TGF-β1. Although we do not yet fully understand why the context for $PGE_2$ signaling is different in the presence and absence of TGF-β1, it may, in part, reflect differential cell-cell signaling related to adherens junctions. Our unpublished observations suggest that TGF-β1 treatment diminishes expression of the adherens junction protein, zonula occludens (ZO)-1α, whereas $PGE_2$ has no influence on this protein when added alone or in combination with TGF-β1. Thus differences such as this may contribute to the differential cellular context for $PGE_2$ signaling in the presence and absence of TGF-β1. It is also possible that the distribution of transcriptional coactivators may also be different in the presence and absence of $PGE_2$. For instance, $PGE_2$-mediated signaling phosphorylates CREB and activates MAP kinases much faster than TGF-β1-mediated signaling can activate Smads. As such, it is likely that in the presence of $PGE_2$, available transcription factors may be preferentially sequestered for CREB-mediated or activator protein-1-dependent transcription as opposed to Smad-mediated transcription. Similarly, the later inhibition of MAP kinase signaling by $PGE_2$ may prevent Smad-mediated transcription at the 24-h time point. Additionally, Rho/Rac/Cdc42-dependent signaling pathways need to be investigated. These questions will be the focus of our future work.

Adhesion-generated signaling and Y-397 phosphorylation of FAK is a prerequisite for TGF-β1-induced fibroblast to myofibroblast transformation (41). The present investigations demonstrate that inhibition of Y-397 phosphorylation of FAK by $PGE_2$ in the presence of TGF-β1 is associated with decreased myofibroblast differentiation and changes in focal adhesion distribution, cytoskeletal changes, and fibroblast shape in both fetal and adult fibroblasts. Hypophosphorylation of FAK and disassembly of actin stress fibers and focal adhesions by prostacyclin analogs and $PGE_2$ has been reported recently in human aortic smooth muscle cells (4). Thus $PGE_2$ signaling is likely dictated by both cell type and the nature of the costimulation. Our data support the concept that FAK regulates cytoskeletal fluidity, focal adhesions, and cell movement (27). These data are consistent with a role for adhesion signaling in survival, growth, and apoptosis of myofibroblasts (18,22,24,45) and the fact that FAK promotes the organization of fibronectin matrix and fibrillar adhesions (17). These data are further supported by the observation that the stellate morphology induced by cAMP in rat vascular smooth muscle cells is associated with loss of actin stress fibers and focal adhesions (31). We have previously shown the fibronectin accumulation and the increased expression of $\alpha_4$-, $\alpha_5$-, and $\beta_1$-integrins are associated with TGF-β1-induced myofibroblast differentiation (41). The effects of $PGE_2$ on these and other matrix components remain to be investigated.

Myofibroblast differentiation is associated with Akt phosphorylation events. TGF-β1 induced S-473 Akt phosphorylation in human lung fibroblasts at all time points tested. However, this phosphorylation was inhibited by $PGE_2$ within 30 min. This could occur via inhibition of PI3K, activation of PTEN (46), or both. These data suggest that $PGE_2$ is able to limit the prosurvival pathways that are normally active in myofibroblasts. This would imply that $PGE_2$ treatment would render myofibroblasts susceptible to apoptosis as would be expected in normal wound resolution. Certainly, the cytoskeletal changes noted in the presence of $PGE_2$ suggest that the cells may be susceptible to anoikis. However, when we tested IMR-90 cells cultured with TGF-β1 in the presence or absence of $PGE_2$ for 24 h for evidence of alterations in apoptosis, Western blot analysis did not reveal any increase in cleaved caspase-3 expression in the presence of $PGE_2$ during the first 24 h of culture. Thus, if it occurs, induction of apoptosis by $PGE_2$ may require longer exposure times. In fact, our previous studies (15) have suggested inhibition of the Akt pathway induces apoptosis in TGF-β1-treated IMR-90 cells only after 5 days. Another

possibility is that $PGE_2$ may serve to limit myofibroblast differentiation and function without diminishing cell survival.

As mentioned earlier, the cellular context for $PGE_2$ signaling is likely different in the presence and absence of TGF-β1. It is likely that cAMP signaling is compartmentalized within the cell. Thus changes in cell shape may serve to alter the proximity of effectors and targets at the subcellular level. Since many of the effects brought about by $PGE_2$ occur within minutes (rapid activation of MAP kinases or STAT-3), the fibroblast context, its interactions with the environment, and its metabolic state are altered dramatically. Thus the conditions required for TGF-β1 to bring about the differentiation of fibroblasts to myofibroblasts no longer exist in the presence of $PGE_2$. The temporal onset of phosphorylation of MAP kinases by $PGE_2$ or TGF-β1 is strikingly different. $PGE_2$ is able to phosphorylate all members of the MAP kinase family within 5 min, whereas the effect of TGF-β1 is delayed. It is possible that the MAP kinases activated by $PGE_2$ may influence pathways that are distinct from pathways stimulated by the activation of MAP kinases with TGF-β1. These investigations point to the importance of stimulus-specific dynamic activation of MAP kinases with respect to time of onset and subcellular localization (30).

Our research has determined that $PGE_2$ signaling inhibits adhesion-dependent signaling (paxillin, STAT-3, FAK, and Akt) necessary for fibroblast-to-myofibroblast transformation to occur. $PGE_2$ signaling does not prevent the TGF-β1-induced activation or translocation of Smad2/3/4 to the nucleus. Additionally, $PGE_2$ coadministration alters the kinetics of MAP kinase activation. Although the inhibitory effects of $PGE_2$ may be mediated by any or all of these actions on TGF-β1 signaling, we think it likely that inhibition of FAK activation is critical. We (41) have previously shown that FAK inhibition can limit TGF-β1-induced differentiation of fetal fibroblasts to myofibroblasts. Our current data link the actions of $PGE_2$ to inhibition of FAK in both fetal and adult lung fibroblasts. Further characterizations of the inhibitory signaling pathways induced by $PGE_2$ may identify potential new targets for therapeutic manipulation.

## Acknowledgments

**GRANTS**

This work was supported by National Heart, Lung, and Blood Institute Grants HL-071586 (B. B. Moore), P50-HL-56402 (B. B. Moore and M. Peters-Golden), HL-06767 (V. J. Thannickal), P50-HL-074024 (V. J. Thannickal), and K08-HL-070990 (E. S. White).

## REFERENCES

1. Bhattacharyya S, Ghosh AK, Pannu J, Mori Y, Takagawa S, Chen G, Trojanowska M, Gilliam AC, Varga J. Fibroblast expression of the coactivator p300 governs the intensity of profibrotic response to transforming growth factor beta. Arthritis Rheum 2005;52:1248–1258. [PubMed: 15818659]
2. Border WA, Noble NA. Transforming growth factor beta in tissue fibrosis. N Engl J Med 1994;331:1286–1292. [PubMed: 7935686]
3. Border WA, Ruoslahti E. Transforming growth factor-beta in disease: the dark side of tissue repair. J Clin Invest 1992;90:1–7. [PubMed: 1634602]
4. Bulin C, Albrecht U, Bode JG, Weber AA, Schror K, Levkau B, Fischer JW. Differential effects of vasodilatory prostaglandins on focal adhesions, cytoskeletal architecture, and migration in human aortic smooth muscle cells. Arterioscler Thromb Vasc Biol 2005;25:84–89. [PubMed: 15458982]
5. Charbeneau RP, Christensen PJ, Chrisman CJ, Paine R, Toews GB, Peters-Golden M, Moore BB. Impaired synthesis of prostaglandin $E_2$ by lung fibroblasts and alveolar epithelial cells from GM-CSF $^{-/-}$mice: implications for fibroproliferation. Am J Physiol Lung Cell Mol Physiol 2003;284:L1103–L1111. [PubMed: 12598228]

6. Darby I, Skalli O, Gabbiani G. Alpha-smooth muscle actin is transiently expressed by myofibroblasts during experimental wound healing. Lab Invest 1990;63:21–29. [PubMed: 2197503]
7. Desmouliere A, Geinoz A, Gabbiani F, Gabbiani G. Transforming growth factor-beta 1 induces alpha-smooth muscle actin expression in granulation tissue myofibroblasts and in quiescent and growing cultured fibroblasts. J Cell Biol 1993;122:103–111. [PubMed: 8314838]
8. Desmouliere A, Redard M, Darby I, Gabbiani G. Apoptosis mediates the decrease in cellularity during the transition between granulation tissue and scar. Am J Pathol 1995;146:56–66. [PubMed: 7856739]
9. Friedman A, Perrimon N. A functional RNAi screen for regulators of receptor tyrosine kinase and ERK signalling. Nature 2006;444:230–234. [PubMed: 17086199]
10. Ghosh AK, Bhattacharyya S, Varga J. The tumor suppressor p53 abrogates Smad-dependent collagen gene induction in mesenchymal cells. J Biol Chem 2004;279:47455–47463. [PubMed: 15345715]
11. Han JD, Rubin CS. Regulation of cytoskeleton organization and paxillin dephosphorylation by cAMP. Studies on murine Y1 adrenal cells. J Biol Chem 1996;271:29211–29215. [PubMed: 8910579]
12. Hashimoto S, Gon Y, Takeshita I, Matsumoto K, Maruoka S, Horie T. Transforming growth factor-beta1 induces phenotypic modulation of human lung fibroblasts to myofibroblast through a c-Jun-$NH_2$-terminal kinase-dependent pathway. Am J Respir Crit Care Med 2001;163:152–157. [PubMed: 11208641]
13. Hodges RJ, Jenkins RG, Wheeler-Jones CP, Copeman DM, Bottoms SE, Bellingan GJ, Nanthakumar CB, Laurent GJ, Hart SL, Foster ML, McAnulty RJ. Severity of lung injury in cyclooxygenase-2-deficient mice is dependent on reduced prostaglandin $E_2$ production. Am J Pathol 2004;165:1663–1676. [PubMed: 15509536]
14. Horowitz JC, Cui Z, Moore TA, Meier TR, Reddy RC, Toews GB, Standiford TJ, Thannickal VJ. Constitutive activation of prosurvival signaling in alveolar mesenchymal cells isolated from patients with non-resolving acute respiratory distress syndrome. Am J Physiol Lung Cell Mol Physiol 2006;290:L415–L425. [PubMed: 16214815]
15. Horowitz JC, Lee DY, Waghray M, Keshamouni VG, Thomas PE, Zhang H, Cui Z, Thannickal VJ. Activation of the pro-survival phosphatidylinositol 3-kinase/AKT pathway by transforming growth factor-beta1 in mesenchymal cells is mediated by p38 MAPK-dependent induction of an autocrine growth factor. J Biol Chem 2004;279:1359–1367. [PubMed: 14576166]
16. Huang SK, Wettlaufer SH, Hogaboam CM, Aronoff DM, Peters-Golden M. Prostaglandin $E_2$ inhibits collagen expression and proliferation in patient-derived normal lung fibroblasts via E prostanoid 2 receptor and cAMP signaling. Am J Physiol Lung Cell Mol Physiol 2007;292:L405–L413. [PubMed: 17028262]
17. Ilic D, Kovacic B, Johkura K, Schlaepfer DD, Tomasevic N, Han Q, Kim JB, Howerton K, Baumbusch C, Ogiwara N, Streblow DN, Nelson JA, Dazin P, Shino Y, Sasaki K, Damsky CH. FAK promotes organization of fibronectin matrix and fibrillar adhesions. J Cell Sci 2004;117:177–187. [PubMed: 14657279]
18. Ingber DE. Tensegrity II. How structural networks influence cellular information processing networks. J Cell Sci 2003;116:1397–1408. [PubMed: 12640025]
19. Keerthisingam CB, Jenkins RG, Harrison NK, Hernandez-Rodriguez NA, Booth H, Laurent GJ, Hart SL, Foster ML, McAnulty RJ. Cyclooxygenase-2 deficiency results in a loss of the anti-proliferative response to transforming growth factor-beta in human fibrotic lung fibroblasts and promotes bleomycin-induced pulmonary fibrosis in mice. Am J Pathol 2001;158:1411–1422. [PubMed: 11290559]
20. Khalil N, Xu YD, O'Connor R, Duronio V. Proliferation of pulmonary interstitial fibroblasts is mediated by transforming growth factor-beta1-induced release of extracellular fibroblast growth factor-2 and phosphorylation of p38 MAPK and JNK. J Biol Chem 2005;280:43000–43009. [PubMed: 16246848]
21. Kolodsick JE, Peters-Golden M, Larios J, Toews GB, Thannickal VJ, Moore BB. Prostaglandin $E_2$ inhibits fibroblast to myofibroblast transition via E prostanoid receptor 2 signaling and cyclic adenosine monophosphate elevation. Am J Respir Cell Mol Biol 2003;29:537–544. [PubMed: 12738687]
22. Kumar S, Maxwell IZ, Heisterkamp A, Polte TR, Lele TP, Salanga M, Mazur E, Ingber DE. Viscoelastic retraction of single living stress fibers and its impact on cell shape, cytoskeletal

organization and extracellular matrix mechanics. Biophys J 2006;90:3762–3773. [PubMed: 16500961]

23. Lamb NJ, Fernandez A, Conti MA, Adelstein R, Glass DB, Welch WJ, Feramisco JR. Regulation of actin microfilament integrity in living nonmuscle cells by the cAMP-dependent protein kinase and the myosin light chain kinase. J Cell Biol 1988;106:1955–1971. [PubMed: 3290222]
24. Lele TP, Pendse J, Kumar S, Salanga M, Karavitis J, Ingber DE. Mechanical forces alter zyxin unbinding kinetics within focal adhesions of living cells. J Cell Physiol 2006;207:187–194. [PubMed: 16288479]
25. Majno G, Gabbiani G, Hirschel BJ, Ryan GB, Statkov PR. Contraction of granulation tissue in vitro: similarity to smooth muscle. Science 1971;173:548–550. [PubMed: 4327529]
26. Massague J, Seoane J, Wotton D. Smad transcription factors. Genes Dev 2005;19:2783–2810. [PubMed: 16322555]
27. Mitra SK, Hanson DA, Schlaepfer DD. Focal adhesion kinase: in command and control of cell motility. Nat Rev Mol Cell Biol 2005;6:56–68. [PubMed: 15688067]
28. Moore BB, Ballinger MN, White ES, Green ME, Herrygers AB, Wilke CA, Toews GB, Peters-Golden M. Bleomycin-induced E prostanoid receptor changes alter fibroblast responses to prostaglandin $E_2$. J Immunol 2005;174:5644–5649. [PubMed: 15843564]
29. Nakao A, Fujii M, Matsumura R, Kumano K, Saito Y, Miyazono K, Iwamoto I. Transient gene transfer and expression of Smad7 prevents bleomycin-induced lung fibrosis in mice. J Clin Invest 1999;104:5–11. [PubMed: 10393693]
30. Olsen JV, Blagoev B, Gnad F, Macek B, Kumar C, Mortensen P, Mann M. Global, in vivo, and site-specific phosphorylation dynamics in signaling networks. Cell 2006;127:635–648. [PubMed: 17081983]
31. Pelletier S, Julien C, Popoff MR, Lamarche-Vane N, Meloche S. Cyclic AMP induces morphological changes of vascular smooth muscle cells by inhibiting a Rac-dependent signaling pathway. J Cell Physiol 2005;204:412–422. [PubMed: 15706595]
32. Peters-Golden M, Bailie M, Marshall T, Wilke C, Phan SH, Toews GB, Moore BB. Protection from pulmonary fibrosis in leukotriene-deficient mice. Am J Respir Crit Care Med 2002;165:229–235. [PubMed: 11790660]
33. Romashkova JA, Makarov SS. NF-kappaB is a target of AKT in anti-apoptotic PDGF signalling. Nature 1999;401:86–90. [PubMed: 10485711]
34. Rossi AG, McCutcheon JC, Roy N, Chilvers ER, Haslett C, Dransfield I. Regulation of macrophage phagocytosis of apoptotic cells by cAMP. J Immunol 1998;160:3562–3568. [PubMed: 9531319]
35. Silver DL, Naora H, Liu J, Cheng W, Montell DJ. Activated signal transducer and activator of transcription (STAT) 3: localization in focal adhesions and function in ovarian cancer cell motility. Cancer Res 2004;64:3550–3558. [PubMed: 15150111]
36. Sime PJ, Xing Z, Graham FL, Csaky KG, Gauldie J. Adenovector-mediated gene transfer of active transforming growth factor-beta1 induces prolonged severe fibrosis in rat lung. J Clin Invest 1997;100:768–776. [PubMed: 9259574]
37. Simonsson M, Kanduri M, Gronroos E, Heldin CH, Ericsson J. The DNA binding activities of Smad2 and Smad3 are regulated by coactivator-mediated acetylation. J Biol Chem 2006;281:39870–39880. [PubMed: 17074756]
38. Skalli, O.; Gabbiani, G. The biology of the myofibroblast: relationship to wound contraction and fibrocontractive diseases. In: Clark, RA.; Henson, PM., editors. The Molecular and Cellular Biology of Wound Repair. New York: Plenum; 1988. p. 373-402.
39. Skalli O, Ropraz P, Trzeciak A, Benzonana G, Gillessen D, Gabbiani G. A monoclonal antibody against alpha-smooth muscle actin: a new probe for smooth muscle differentiation. J Cell Biol 1986;103:2787–2796. [PubMed: 3539945]
40. Suzuki H, Uchida K, Nitta K, Nihei H. Role of mitogen-activated protein kinase in the regulation of transforming growth factor-beta-induced fibronectin accumulation in cultured renal interstitial fibroblasts. Clin Exp Nephrol 2004;8:188–195. [PubMed: 15480895]
41. Thannickal VJ, Lee DY, White ES, Cui Z, Larios JM, Chacon R, Horowitz JC, Day RM, Thomas PE. Myofibroblast differentiation by transforming growth factor-beta1 is dependent on cell adhesion

and integrin signaling via focal adhesion kinase. J Biol Chem 2003;278:12384–12389. [PubMed: 12531888]

42. Vancheri C, Mastruzzo C, Tomaselli V, Sortino MA, D'Amico L, Bellistri G, Pistorio MP, Salinaro ET, Palermo F, Mistretta A, Crimi N. Normal human lung fibroblasts differently modulate interleukin-10 and interleukin-12 production by monocytes: implications for an altered immune response in pulmonary chronic inflammation. Am J Respir Cell Mol Biol 2001;25:592–599. [PubMed: 11713101]
43. Vancheri C, Sortino MA, Tomaselli V, Mastruzzo C, Condorelli F, Bellistri G, Pistorio MP, Canonico PL, Crimi N. Different expression of TNF-alpha receptors and prostaglandin $E_2$ production in normal and fibrotic lung fibroblasts: potential implications for the evolution of the inflammatory process. Am J Respir Cell Mol Biol 2000;22:628–634. [PubMed: 10783136]
44. Viatour P, Merville MP, Bours V, Chariot A. Phosphorylation of NF-kappaB and IkappaB proteins: implications in cancer and inflammation. Trends Biochem Sci 2005;30:43–52. [PubMed: 15653325]
45. Wang N, Butler JP, Ingber DE. Mechanotransduction across the cell surface and through the cytoskeleton. Science 1993;260:1124–1127. [PubMed: 7684161]
46. White ES, Atrasz RG, Dickie EG, Aronoff DM, Stambolic V, Mak TW, Moore BB, Peters-Golden M. Prostaglandin $E_2$ inhibits fibroblast migration by E-prostanoid 2 receptor-mediated increase in PTEN activity. Am J Respir Cell Mol Biol 2005;32:135–141. [PubMed: 15539459]
47. Wilborn J, Crofford LJ, Burdick MD, Kunkel SL, Strieter RM, Peters-Golden M. Cultured lung fibroblasts isolated from patients with idiopathic pulmonary fibrosis have a diminished capacity to synthesize prostaglandin $E_2$ and to express cyclooxygenase-2. J Clin Invest 1995;95:1861–1868. [PubMed: 7706493]

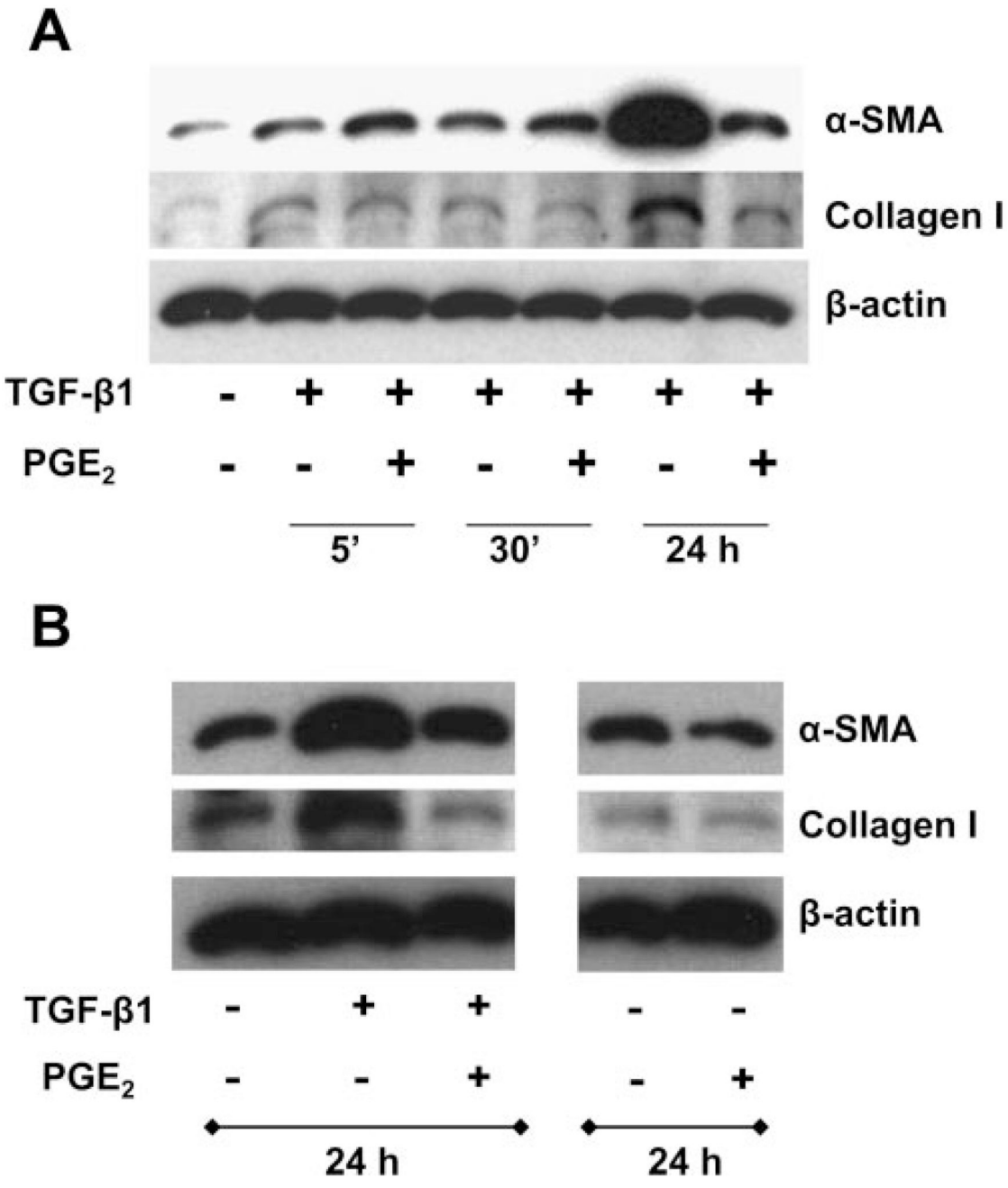


**Fig. 1.**

$PGE_2$ suppresses the expression of collagen and smooth muscle actin-α (α-SMA). *A*: quiescent human lung fibroblasts (IMR-90) were treated with TGF-β1 (2 ng/ml), or TGF-β1 (2 ng/ml) and $PGE_2$ (10 nM), under serum-free conditions for indicated times, and cell lysates were prepared. Cell lysates were subjected to SDS-PAGE followed by immunoblotting with antibodies against collagen 1, α-SMA, and β-actin. *B*: IMR-90 cells were treated with TGF-β1 alone, $PGE_2$ alone (10 nM), or TGF-β1 + $PGE_2$, and cell lysates were analyzed as above after 24 h. Data are representative of 3 independent experiments.

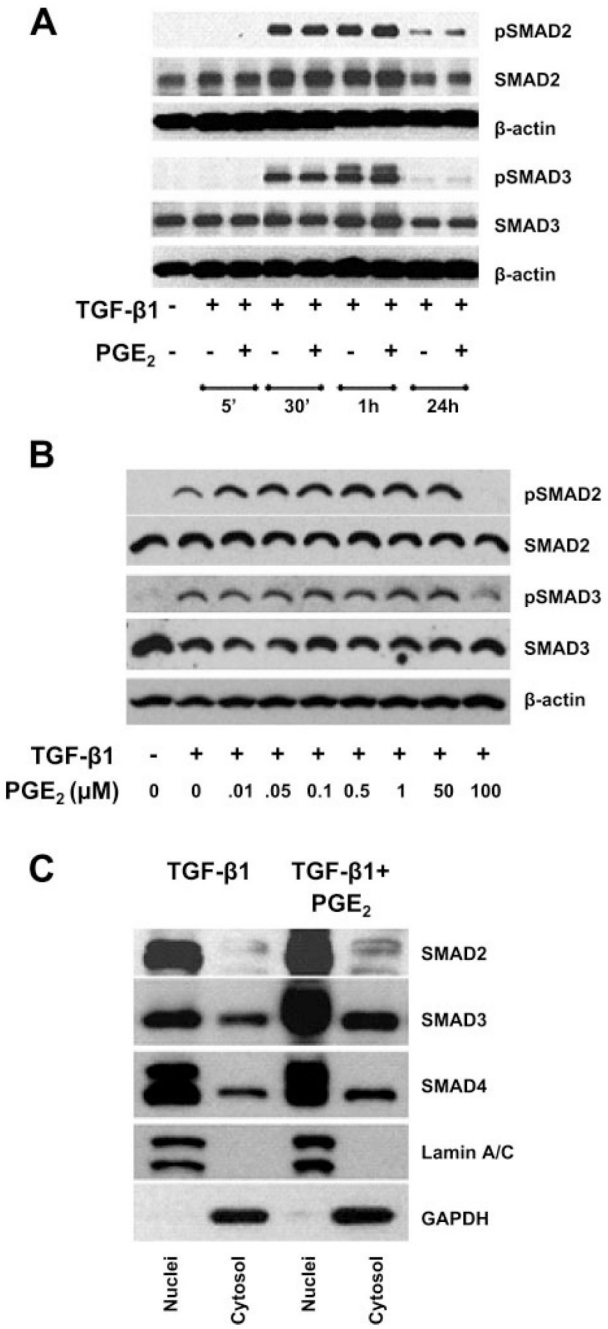


**Fig. 2.**

$PGE_2$ did not affect the TGF-β1-stimulated phosphorylation (p) of Smad2/3. *A*: quiescent human lung fibroblasts (IMR-90) were treated with TGF-β1 (2 ng/ml), or TGF-β1 (2 ng/ml) and $PGE_2$ (10 nM), under serum-free conditions, and cell lysates were prepared at the times indicated. Cell lysates were subjected to SDS-PAGE followed by immunoblotting with antibodies against pS465/467 Smad2 and pS422/424 Smad3, Smad2, and Smad3. Blots were probed first with phospho-specific Smad antibodies, stripped, and reblotted with antibodies for respective nonphosphorylated Smad proteins or β-actin. *B*: IMR-90 cells were treated as above with TGF-β1 in the presence or absence of increasing concentrations of $PGE_2$ ranging from 0.01 to 100 μM, and phosphorylation of Smad2 and Smad3 was assessed as in *A*. *C*:

$PGE_2$ did not abrogate the translocation of Smad2/3/4 complex to the nucleus in human lung fibroblasts. Quiescent human lung fibroblasts (IMR-90) were treated with TGF-β1 (2 ng/ml), or TGF-β1 (2 ng/ml) and $PGE_2$ (10 nM), under serum-free conditions for 30 min. Cells were lysed, and nuclei and cytosol were fractionated. Reduced nuclear and cytosolic fractions were used for Western blot analysis with antibodies against Smad2, Smad3, and Smad4. GAPDH and lamin A/C were used as markers for cytosol and nuclear fractions, respectively. Data are representative of 3 independent experiments.

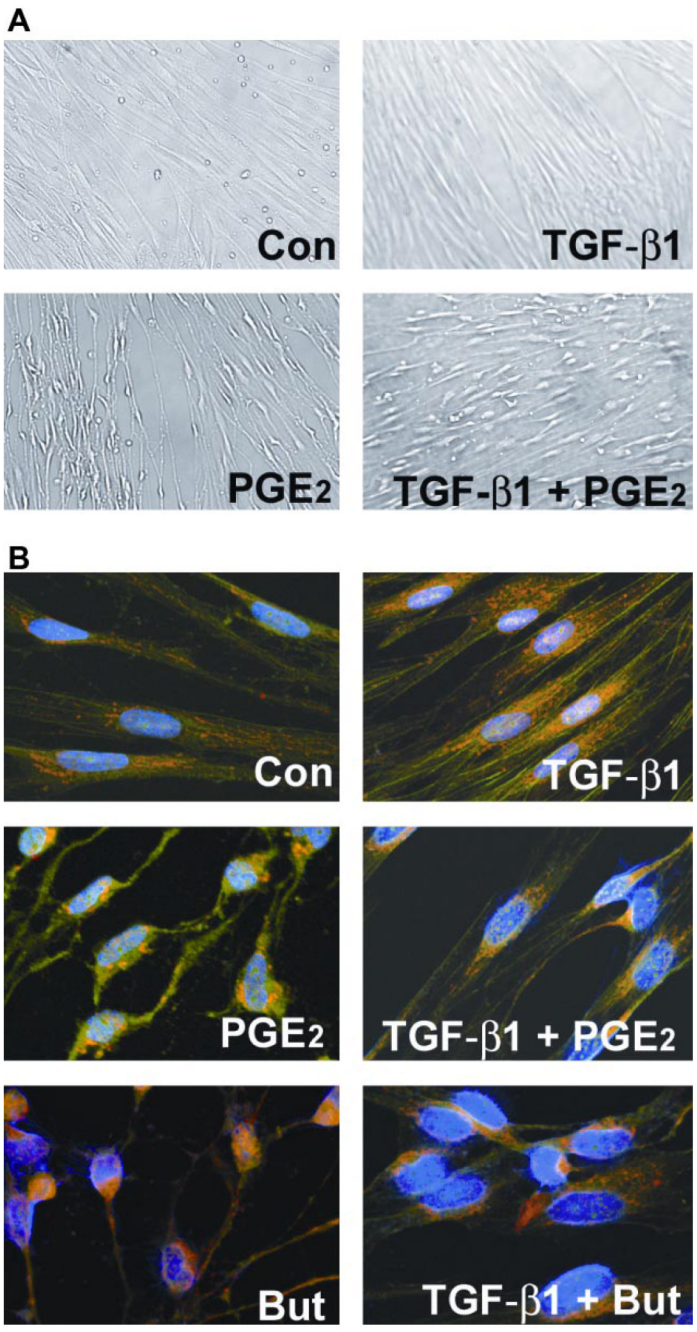


**Fig. 3.**

$PGE_2$ induces sudden and sustained morphological changes. *A*: IMR-90 cells were growth-arrested at 85% confluency for 48 h. Medium was replaced with serum-free media or that containing TGF-β1 (2 ng/ml) or $PGE_2$ (10 nM) or both TGF-β1 and $PGE_2$. Cells were photographed after 5 min of treatment. Control (Con) cells show characteristic flattened spindle shape. TGF-β1-treated cells show spindle shape with a more 3-dimensional appearance. $PGE_2$-treated cells are no longer spindle shaped and appear shrunken longitudinally with decrease in area of surface fibrillar and focal adhesion. The appearance of the cells treated with both TGF-β1 and $PGE_2$ is intermediate between those treated with TGF-β1 alone and those treated with $PGE_2$ alone. *B*: $PGE_2$ alters cytoskeletal structure and focal adhesions in human

lung fibroblasts. Shown are FITC-phalloidin staining (green), immunocytochemistry with paxillin (red), and 4,6-diamidino-2-phenylindole (DAPI) staining of nuclei (blue). IMR-90 cells were serum-deprived for 48 h. Medium was replaced with serum-free media or that containing TGF-β1, $PGE_2$, butaprost (But), or combinations of both TGF-β1 and $PGE_2$ or butaprost. After 24 h, cells were washed, fixed, and stained. Cells were then analyzed using laser-scanning confocal microscopy with appropriate wavelengths using a ×60 water immersion objective. Merged images are shown, and focal adhesions appear as yellow/orange.

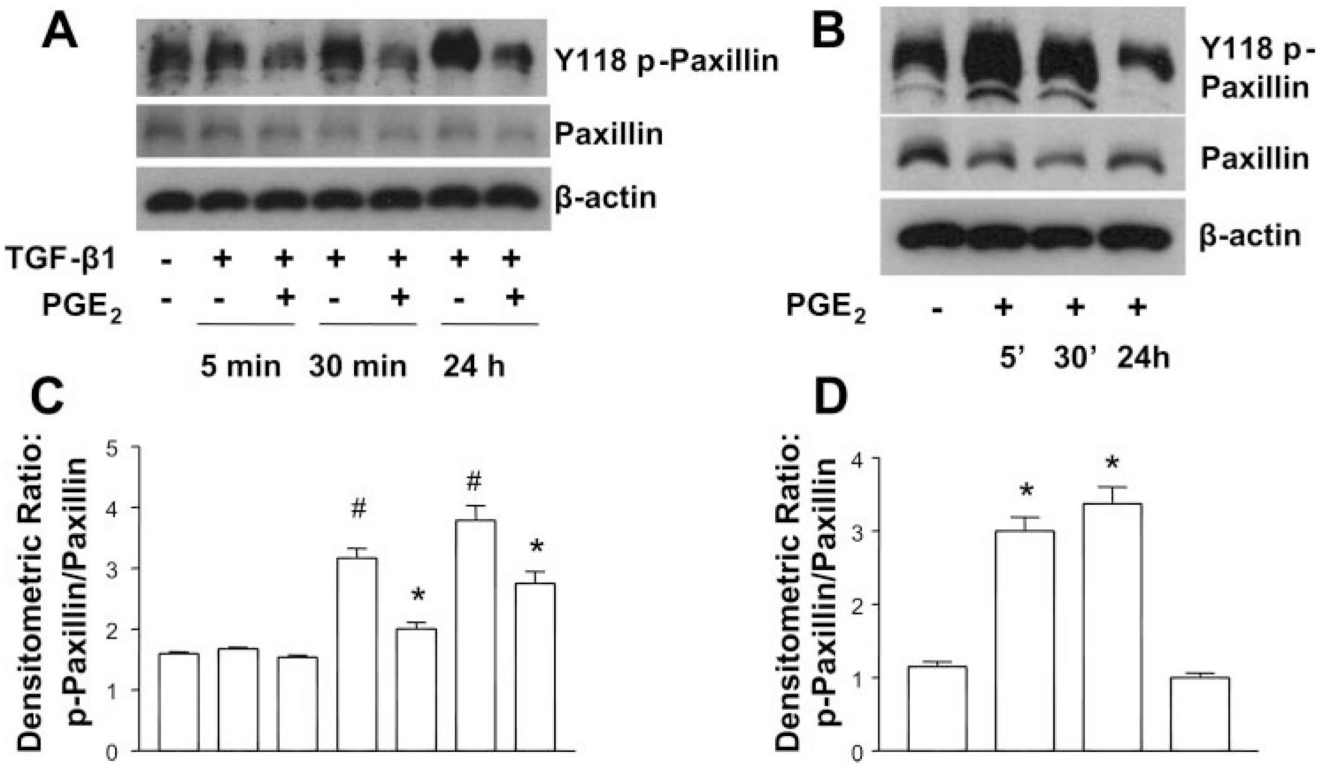


**Fig. 4.**

$PGE_2$ inhibits the TGF-β1-stimulated phosphorylation of paxillin. *A*: quiescent human lung fibroblasts (IMR-90) were treated with TGF-β1 (2 ng/ml), or TGF-β1 (2 ng/ml) and $PGE_2$ (10 nM), under serum-free conditions, and cell lysates were prepared at the times indicated. *B*: quiescent human lung fibroblasts (IMR-90) were treated with $PGE_2$ (10 nM) under serum-free conditions, and cell lysates were prepared at the times indicated. Cell lysates were subjected to SDS-PAGE followed by immunoblotting with antibodies against p-paxillin. Blots probed with antibody against p-paxillin were stripped and blotted with antibodies against paxillin and β-actin sequentially. *C*: densitometry data for $n = 3$ experiments as in *A*. #$P < 0.05$ for TGF-β1-treated samples compared with untreated control; *$P < 0.05$ for TGF-β1 + $PGE_2$-treated samples compared with TGF-β1 treatment alone. *D*: densitometry data for $n = 3$ experiments as in *B*. *$P < 0.05$ compared with untreated control.

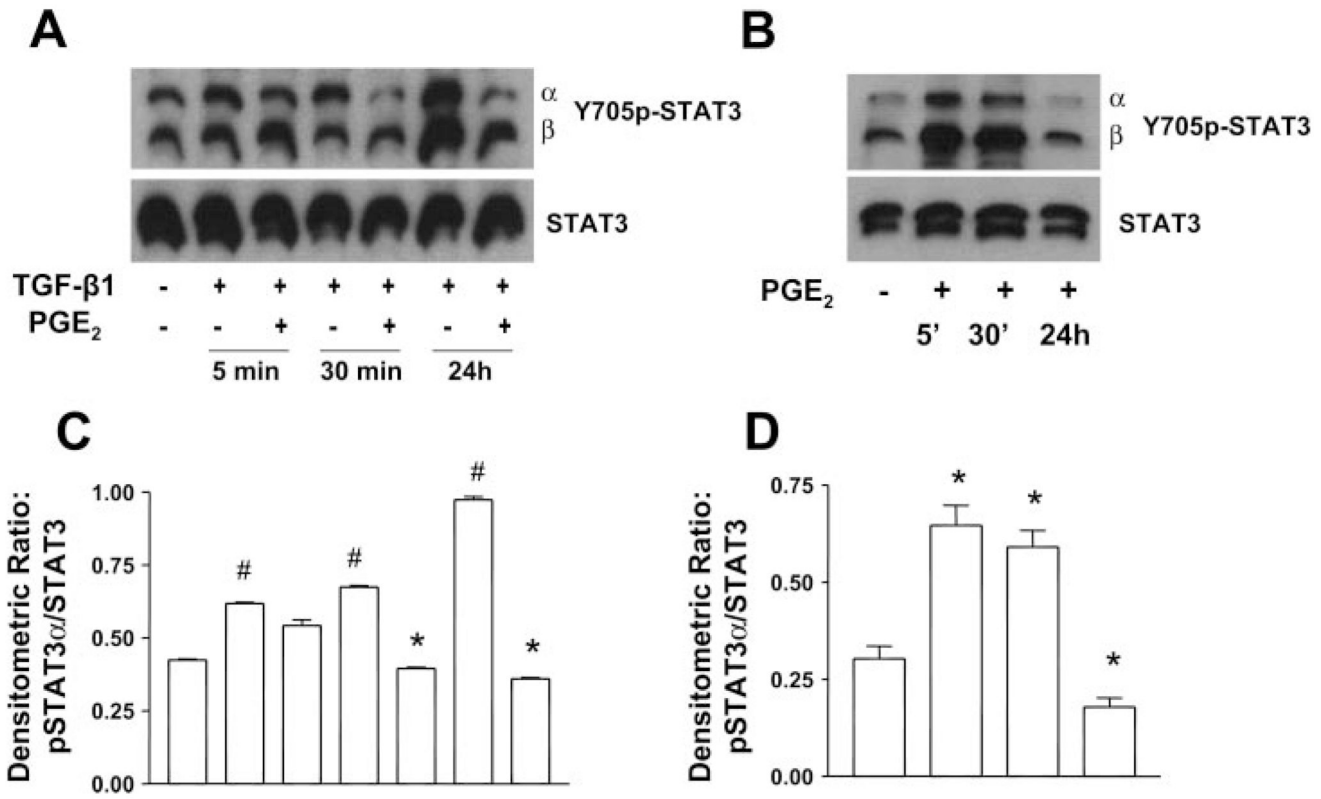


**Fig. 5.**

$PGE_2$ inhibits TGF-β1-stimulated phosphorylation of STAT-3 (Y705p-STAT-3). *A*: quiescent human lung fibroblasts (IMR-90) were treated with TGF-β1 (2 ng/ml), or TGF-β1 (2 ng/ml) and $PGE_2$ (10 nM), under serum-free conditions, and cell lysates were prepared at the times indicated. *B*: quiescent human lung fibroblasts (IMR-90) were treated with $PGE_2$ (10 nM) under serum-free conditions, and cell lysates were prepared at the times indicated. Cell lysates were subjected to SDS-PAGE followed by immunoblotting with antibodies against Y705p-STAT-3, which can detect both the alpha (α) and beta (β) splice forms. Blots probed with antibody against Y705p-STAT-3 were stripped and blotted with antibodies against STAT-3 sequentially. *C*: densitometry data for $n = 3$ experiments as in *A*. *D*: densitometry data for $n = 3$ experiments as in *B*. Significance is indicated with # and * symbols as in Fig 4.

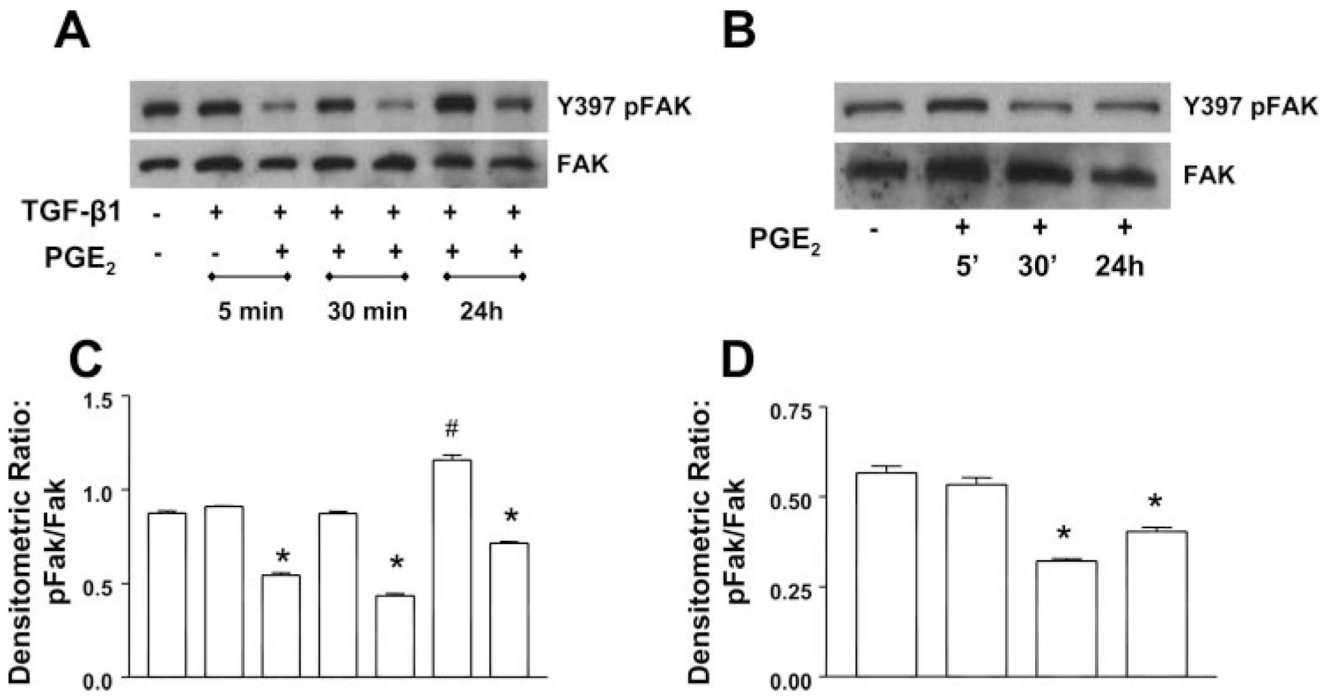


**Fig. 6.**

$PGE_2$ inhibits the TGF-β1-stimulated Y-397 focal adhesion kinase (FAK) autophosphorylation (Y397pFAK). *A*: quiescent human lung fibroblasts (IMR-90) were treated with TGF-β1 (2 ng/ml), or TGF-β1 (2 ng/ml) and $PGE_2$ (10 nM), under serum-free conditions, and cell lysates were prepared at the times indicated. *B*: quiescent human lung fibroblasts (IMR-90) were treated with $PGE_2$ (10 nM) under serum-free conditions, and cell lysates were prepared at the times indicated. Cell lysates were subjected to SDS-PAGE followed by immunoblotting with antibodies against Y397pFAK. Blots probed with antibody against Y397pFAK were stripped and blotted with antibodies against FAK sequentially. *C*: densitometry data for $n = 3$ experiments as in *A*. *D*: densitometry data for $n = 3$ experiments as in *B*. Significance is indicated with # and * symbols as in Fig 4.

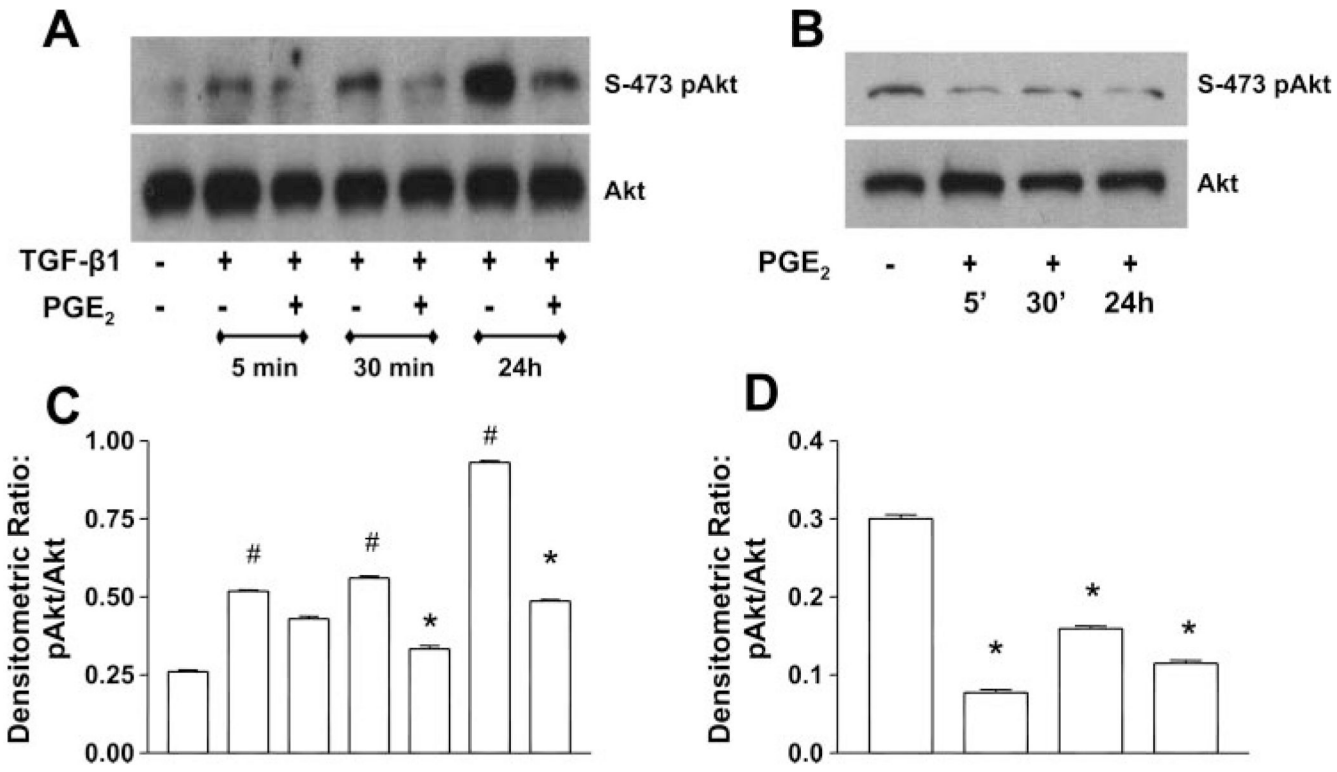


**Fig. 7.**

$PGE_2$ inhibits the TGF-β1-stimulated PKB/Akt phosphorylation. *A*: quiescent human lung fibroblasts (IMR-90) were treated with TGF-β1 (2 ng/ml), or TGF-β1 (2 ng/ml) and $PGE_2$ (10 nM), under serum-free conditions, and cell lysates were prepared at the times indicated. *B*: quiescent human lung fibroblasts (IMR-90) were treated with $PGE_2$ (10 nM) under serum-free conditions, and cell lysates were prepared at the times indicated. Cell lysates were subjected to SDS-PAGE followed by immunoblotting with antibodies against phosphorylated Akt (S-473p-Akt). Blots probed with antibody against S-473p-Akt were stripped and blotted with antibodies against Akt sequentially. *C*: densitometry data for $n = 3$ experiments as in *A*. *D*: densitometry data for $n = 3$ experiments as in *B*. Significance is indicated with # and * symbols as in Fig 4.

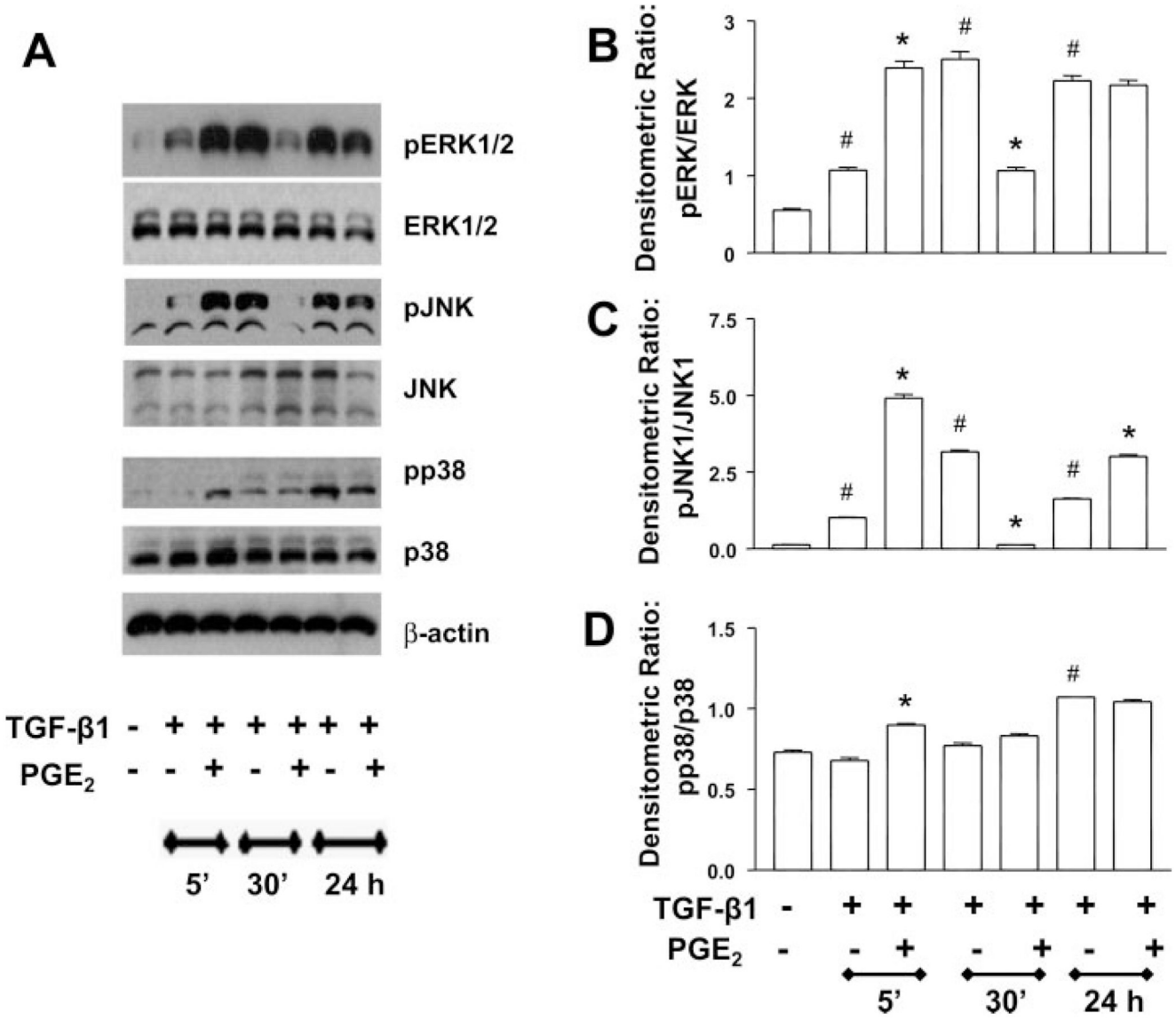


**Fig. 8.**

$PGE_2$ alters the kinetics of TGF-β1-stimulated MAP kinase activation. *A*: quiescent human lung fibroblasts (IMR-90) were treated with TGF-β1 (2 ng/ml), or TGF-β1 (2 ng/ml) and $PGE_2$ (10 nM), under serum-free conditions, and cell lysates were prepared at the times indicated. Cell lysates were subjected to SDS-PAGE followed by immunoblotting with antibodies against pERK1/2, pJNK, or pp38. Blots were then stripped and blotted with antibodies against ERK1/2, JNK, or p38 sequentially. *B*: densitometry data for $n = 3$ experiments looking at ERK phosphorylation. *C*: densitometry data for $n = 3$ experiments looking at JNK phosphorylation. *D*: densitometry data for $n = 3$ experiments looking at p38 phosphorylation. Significance is indicated with # and * symbols as in Fig 4.

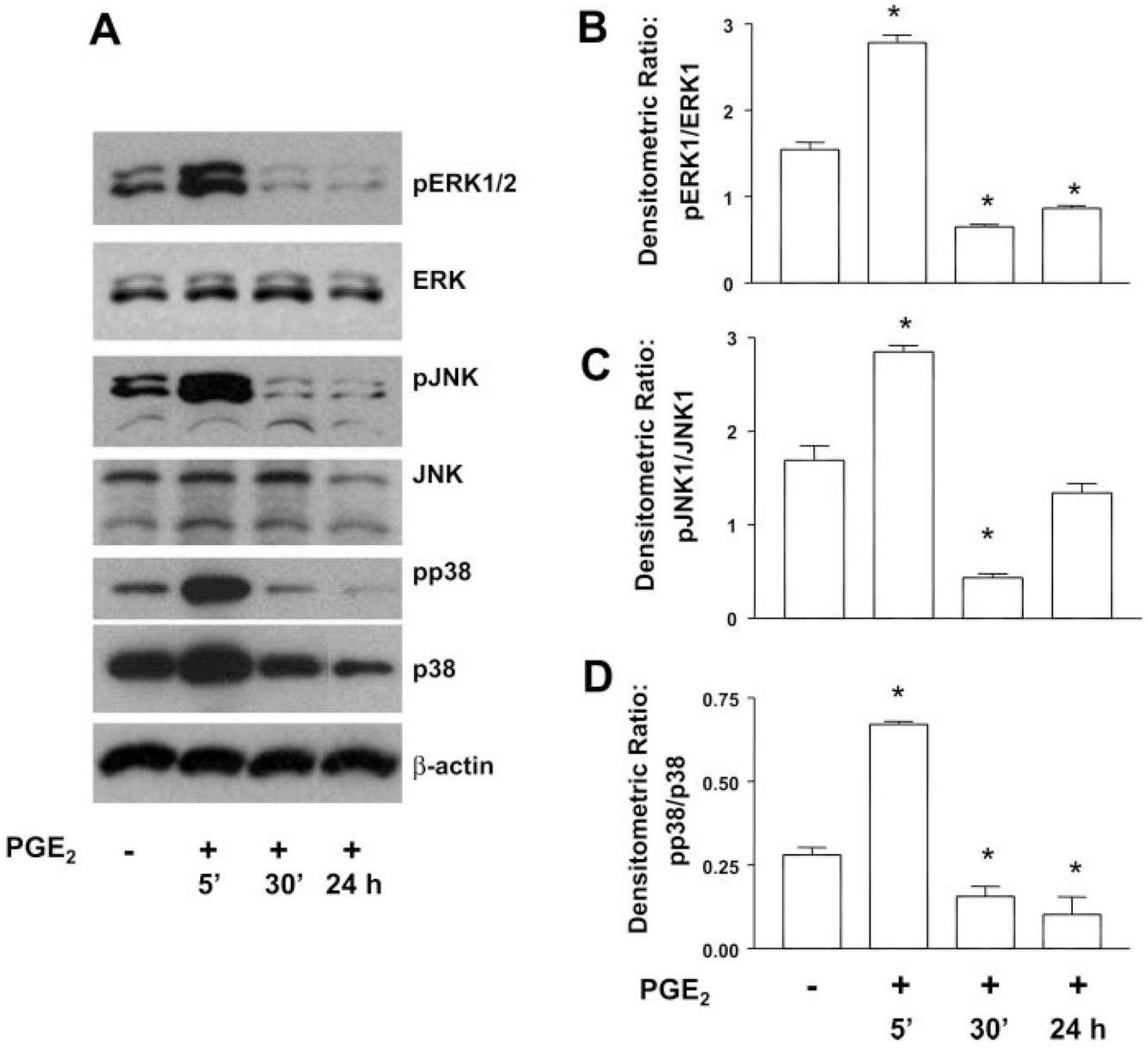


**Fig. 9.**

$PGE_2$ stimulates rapid transient MAP kinase activation but diminished late activation. *A*: quiescent human lung fibroblasts (IMR-90) were treated with $PGE_2$ (10 nM) under serum-free conditions, and cell lysates were prepared at the times indicated. Cell lysates were subjected to SDS-PAGE followed by immunoblotting with antibodies against pERK1/2, pJNK, or pp38. Blots were then stripped and blotted with antibodies against ERK1/2, JNK, or p38 sequentially. *B*: densitometry data for $n = 3$ experiments looking at ERK phosphorylation. *C*: densitometry data for $n = 3$ experiments looking at JNK phosphorylation. *D*: densitometry data for $n = 3$ experiments looking at p38 phosphorylation. $^*P < 0.05$ compared with untreated controls.

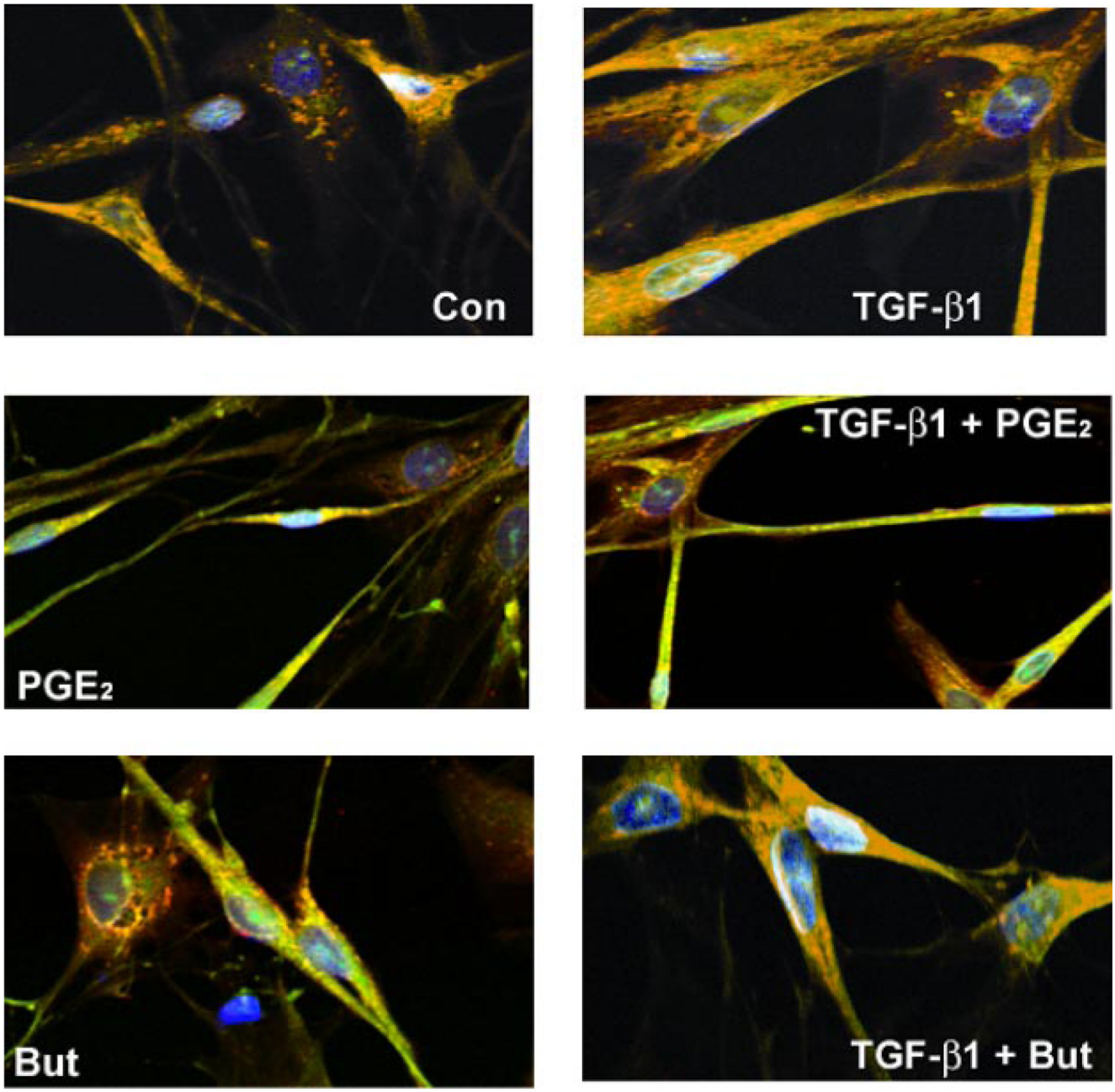


**Fig. 10.**

$PGE_2$ alters cell morphology and inhibits the formation of TGF-β1-induced focal adhesions in adult lung fibroblasts. Normal adult lung fibroblasts were serum-starved for 48 h before culture with serum-free media alone, TGF-β1 alone (2 ng/ml), $PGE_2$ alone (100 nM), butaprost alone (5 μM), or TGF-β1 in combination with $PGE_2$ or butaprost. Cells were then fixed and stained with FITC-phalloidin (green), paxillin (red), and DAPI staining of nuclei (blue). Cells were then analyzed using laser-scanning confocal microscopy with appropriate wavelengths using a ×60 water immersion objective. Merged images are shown, and focal adhesions appear as orange/yellow. Z-stack analysis confirmed the colocalization of the FITC and indocarbocyanine (Cy3) staining.

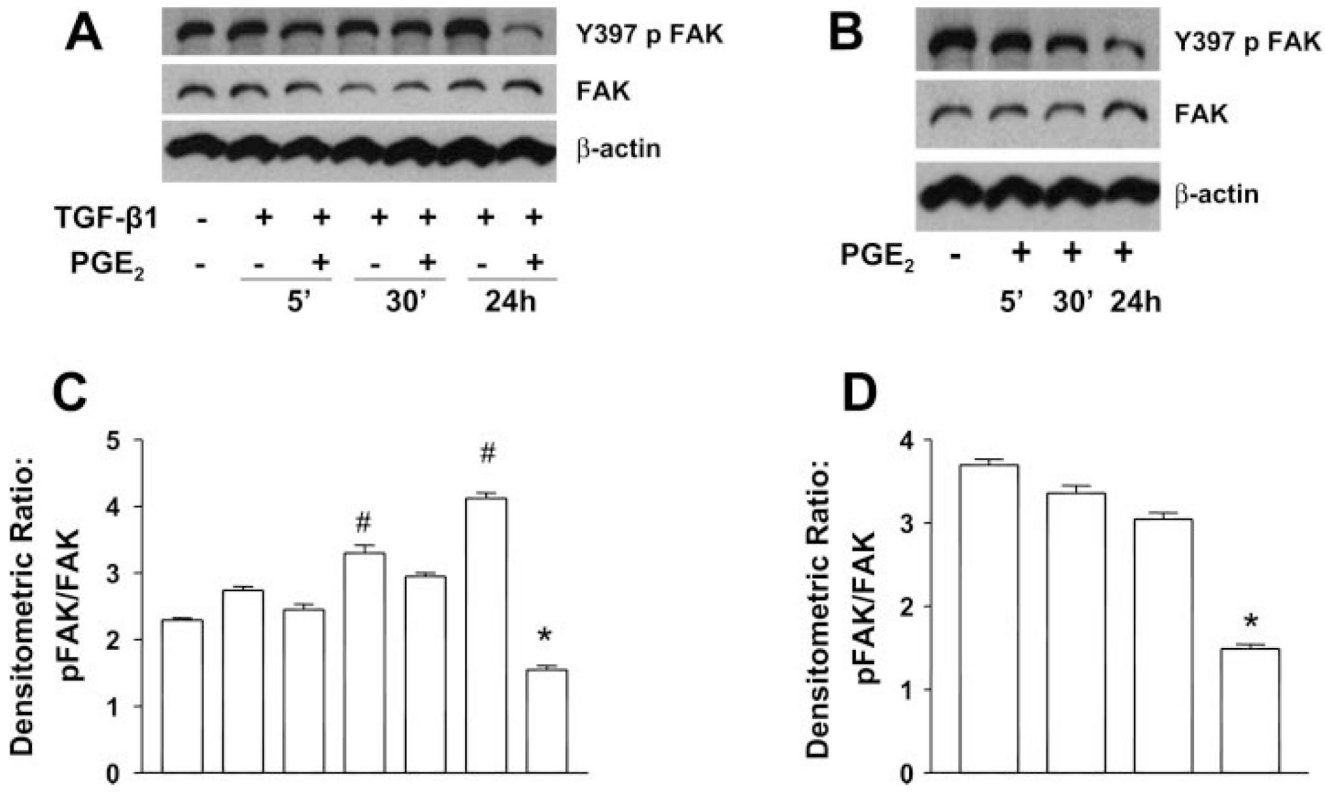


**Fig. 11.**

$PGE_2$ inhibits the TGF-β1-stimulated Y-397 FAK autophosphorylation in adult lung fibroblasts. *A*: quiescent adult lung fibroblasts were treated with TGF-β1 (2 ng/ml), or TGF-β1 (2 ng/ml) and $PGE_2$ (100 nM), under serum-free conditions, and cell lysates were prepared at the times indicated. *B*: quiescent adult lung fibroblasts were treated with $PGE_2$ (100 nM) under serum-free conditions, and cell lysates were prepared at the times indicated. Cell lysates were subjected to SDS-PAGE followed by immunoblotting with antibodies against Y397pFAK. Blots probed with antibody against Y397pFAK were stripped and blotted with antibodies against total FAK sequentially. *C*: densitometry data for $n = 3$ experiments as in *A*. *D*: densitometry data for $n = 3$ experiments as in *B*. Significance is indicated with # and * symbols as in Fig 4.